A centriole- and RanGTP-independent spindle assembly pathway in meiosis I of vertebrate oocytes

Julien Dumont,[1] Sebastian Petri,[2] Franz Pellegrin,[1] Marie-Emilie Terret,[1] Markus T. Bohnsack,[2] Pascale Rassinier,[1] Virginie Georget,[3] Petr Kalab,[4] Oliver J. Gruss,[2] and Marie-Hélène Verlhac[1]

[1]UMR7622, Centre National de la Recherche Scientifique/Université Pierre et Marie Curie, 75005 Paris, France
[2]Zentrum für Molekulare Biologie der Universität Heidelberg, 69120 Heidelberg, Germany
[3]Institut de Biologie Intégrative, IFR83, 75005 Paris, France
[4]Department of Molecular and Cell Biology, University of California, Berkeley, Berkeley, CA 94720

Spindle formation is essential for stable inheritance of genetic material. Experiments in various systems indicate that Ran GTPase is crucial for meiotic and mitotic spindle assembly. Such an important role for Ran in chromatin-induced spindle assembly was initially demonstrated in *Xenopus laevis* egg extracts. However, the requirement of RanGTP in living meiotic cells has not been shown. In this study, we used a fluorescence resonance energy transfer probe to measure RanGTP-regulated release of importin β. A RanGTP-regulated gradient was established during meiosis I and was centered on chromosomes throughout mouse meiotic maturation. Manipulating levels of RanGTP in mice and *X. laevis* oocytes did not inhibit assembly of functional meiosis I spindles. However, meiosis II spindle assembly did not tolerate changes in the level of RanGTP in both species. These findings suggest that a mechanism common to vertebrates promotes meiosis I spindle formation in the absence of chromatin-induced microtubule production and centriole-based microtubule organizing centers.

Introduction

Understanding how microtubules (MTs) reorganize during the cell cycle to assemble into a bipolar spindle is a classic problem of cell biology. Mitotic and meiotic spindles are highly dynamic structures, which assemble around chromosomes or sister chromatids and distribute them into each daughter cell. Errors in spindle assembly lead to severe DNA damage and aneuploidies, responsible for various forms of cancer. Therefore, it is essential that bipolar spindle assembly occurs correctly. Two pathways cooperate to assemble bipolar spindles. One pathway involves centrosomes, which generate astral MTs that continuously search for chromosomes. This is the "search-and-capture" model, which was postulated by Kirschner and Mitchison (1986).

Accumulating evidence suggests that the small GTPase Ran is also a key player in the spatial control of spindle formation during the M phase (for reviews see Gruss and Vernos, 2004; Zheng, 2004; Ciciarello and Lavia, 2005). Production of RanGTP depends on the activity of the regulator of chromosome condensation (RCC1), Ran's nucleotide exchange factor. RCC1 remains bound to chromosomes during the M phase. Thus, it was originally proposed that a high concentration of RanGTP around chromosomes acts as a local switch for spindle assembly (Carazo-Salas et al., 1999; Kalab et al., 1999). This hypothesis has been validated for spindles assembled in vitro and for those assembled in somatic cells. In these systems, higher levels of RanGTP have been detected near chromosomes than in regions distant from chromatin, as indicated by fluorescence resonance energy transfer (FRET) and fluorescence lifetime imaging microscopy techniques (Kalab et al., 2002, 2006; Li and Zheng, 2004).

Experiments in the cell-free system of *Xenopus laevis* initially demonstrated a central role for RanGTP in centrosome-dependent MT production and in chromatin-induced, centrosome-independent spindle assembly (Kalab et al., 1999; Ohba et al., 1999; Wilde and Zheng, 1999; Zhang et al., 1999). High levels of RanGTP stimulate the nucleating capacity of centrosomes but are not essential for basic centrosome nucleation activity. In contrast, chromatin-mediated MT formation depends entirely on the presence of RanGTP in the cell-free system

Correspondence to Marie-Hélène Verlhac: Marie-Helene.Verlhac@snv.jussieu.fr

M.-E. Terret's present address is Memorial Sloan-Kettering Cancer Center, New York, NY 10021.

M.T. Bohnsack's present address is Wellcome Trust Centre for Cell Biology, University of Edinburgh, Edinburgh Eh9 3JR, Scotland, UK.

Abbreviations used in this paper: CSF, cytostatic factor; dbcAMP, dibutiryl cAMP; FRET, fluorescence resonance energy transfer; GV, germinal vesicle; GVBD, GV breakdown; MT, microtubule; MTOC, MT organizing center; RCC1, regulator of chromosome condensation.

The online version of this article contains supplemental material.

The Journal of Cell Biology, Vol. 176, No. 3, January 29, 2007 295–305
http://www.jcb.org/cgi/doi/10.1083/jcb.200605199

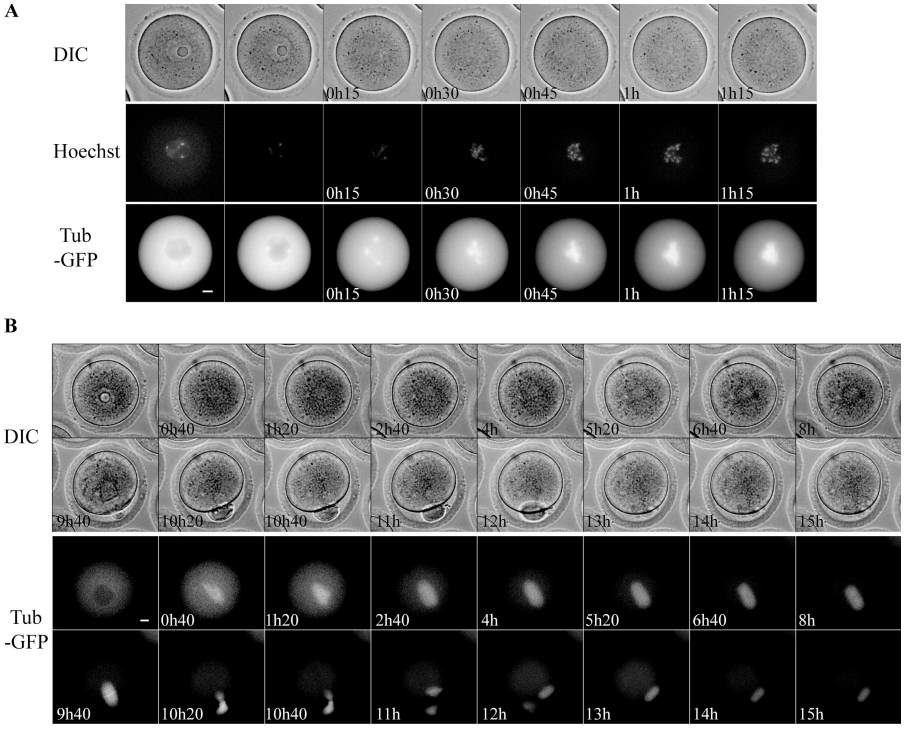

Figure 1. **Spindle formation during mouse meiotic maturation.** (A) Time-lapse microscopy of phase contrast (DIC), Hoechst-stained chromosomes (Hoechst), and tubulin-GFP RNA-injected (Tub-GFP) oocytes. Images were taken every 15 min. (B) Time-lapse microscopy of phase contrast (DIC) and tubulin-GFP RNA-injected (Tub-GFP) oocytes. Images were taken every 20 min. Times after GVBD are indicated in the bottom left corner. $n = 33$. Bars, 10 μm.

(Carazo-Salas et al., 1999). More recently, siRNA experiments and microinjections in living cells of *Caenorhabditis elegans*, *Drosophila melanogaster*, and humans demonstrated that the presence of RanGTP is required for essential functions in spindle formation in centrosome-containing systems (Nachury et al., 2001; Askjaer et al., 2002; Bamba et al., 2002; Kalab et al., 2006; Silverman-Gavrila and Wilde, 2006; Tulu et al., 2006). Ran induces MT formation by releasing various spindle assembly factors, including NuMA, TPX2, and HURP, from the inhibitory effect of importins in the vicinity of chromosomes (Gruss et al., 2001; Nachury et al., 2001; Wiese et al., 2001; Koffa et al., 2006; Sillje et al., 2006; Wong and Fang, 2006).

Many studies have focused on elucidating the function of RanGTP in spindle assembly in meiotic *X. laevis* egg extracts. However, there is no in vivo evidence demonstrating the role of RanGTP in meiotic spindle formation in vertebrates. Meiotic spindle assembly in developing vertebrate oocytes occurs in the absence of centrioles (Szollosi et al., 1972; Huchon et al., 1981; Gard et al., 1995). During meiosis, two successive M phases occur without an intermediate S phase to produce haploid gametes. The first meiotic division is reductional with the segregation of homologous chromosomes. The second meiotic division is equational and resembles mitotic division. Cytostatic factor (CSF) then arrests vertebrate oocytes in metaphase II for many hours, until fertilization. In mouse and *X. laevis* oocytes, MTs nucleate around condensing chromosomes and spindles self-organize in the presence of multiple MT organizing centers (MTOCs). In mouse oocytes, chromosomes gather quickly on a broad metaphase plate through interactions of their arms and MTs. Kinetochore–MT interactions are established at the end of the first meiotic M phase (MI) only (Brunet et al., 1999). Therefore, the oocyte model system is useful for the study of acentrosomal spindle assembly and for the assessment of the role of the Ran pathway in meiosis.

We detected the accumulation of RanGTP around the chromosomes during all stages of mouse meiotic maturation with a previously described FRET-based probe for RanGTP-regulated release of importin β cargo molecules (Kalab et al., 2006). The overexpression of Ran mutants in mouse oocytes and the knock down of RCC1 in *X. laevis* oocytes led to assembly of functional meiosis I spindles in the presence of excess or low RanGTP levels. In contrast, meiosis II spindle assembly was strictly dependent on RanGTP levels in both species. In mouse oocytes, we show that meiosis II progression also depended on RanGTP levels. We demonstrate that there is a mechanism that promotes spindle formation in the absence of both chromatin-induced MT production and centriole-based MTOCs.

Results

The mouse first meiotic spindle is assembled from asters of MTs nucleated distantly from the chromosomes

We followed spindle formation during meiotic maturation in mouse oocytes with high temporal resolution. Mouse oocytes are transparent and ideal for time-lapse microscopy. Meiosis resumes spontaneously in mouse oocytes when they are removed from the ovaries. We initially maintained the oocytes in prophase I at the germinal vesicle (GV) stage in dibutiryl cAMP (dbcAMP)–supplemented medium and injected them with RNA encoding GFP-tagged tubulin (tubulin-GFP; Fig. 1). GV breakdown (GVBD) occurred ∼2 h after release from the dbcAMP-containing medium (Table I). MTs were nucleated from asters that were distant from the chromosomes (Fig. 1 A).

Table I. **Timing of GVBD and of PB1 after dbcAMP release of oocytes injected with RNA encoding Ran mutants**

Type of oocyte	GVBD	PB1	Large PB1
			%
Control (n = 33)	1 h 30 min (±3 min)	91.6%/BD + 9 h (±39 min)	—
Wild type (n = 34)	1 h 24 min (±6 min)	87.5%/BD + 9 h (±31 min)	—
T24N (n = 75)	1 h 30 min (±18 min)	77%/BD + 9 h (±17 min)	13.8
Q69L (n = 26)	1 h 29 min (±8 min)	84%/BD + 8 h 33 min (±15 min)	58

Percentage of first polar body extrusion (PB1). Percentage of abnormally large first polar body estimated visually (large PB1).

These randomly distributed asters reorganized around chromosomes into a bipolar barrel-shaped structure ∼2 h after GVBD. The MI spindle migrated along its long axis to the cortex of the oocyte (Verlhac et al., 2000a) and then anaphase occurred, and the first polar body was extruded ∼9 h after GVBD. A metaphase II (MII) spindle rapidly assembled from remaining MTs around sister chromatids and remained stable during arrest (Fig. 1 B).

Ran and its effectors are differentially regulated in mouse and *X. laevis* oocytes

We investigated the potential role of the Ran system during meiosis by assessing the levels of Ran and RCC1 by Western blot analysis. Endogenous Ran and RCC1 were present in immature (GV) and mature (MII) oocyte extracts from mouse and *X. laevis* (Fig. 2). Although RCC1 levels were approximately two times higher in mouse MII oocyte extracts than in GV oocyte extracts (Fig. 2 A, right), this difference was much greater in *X. laevis* oocytes. In these oocytes, the amount of Ran, RanGAP, and RanBP1 were similar in immature and mature eggs, but the amount of RCC1 increased during meiosis resumption (Fig. 2 B). We biochemically analyzed meiosis in the *X. laevis* system and assayed the amounts of RCC1 during in vitro maturation of *X. laevis* oocytes with high temporal resolution by quantitative Western blot analysis and a Cdk1 activity assay. Overall, RCC1 levels were seven times higher beginning with GVBD and reached maximal levels during MII (Fig. 2 B, right).

A broad RanGTP-regulated importin β release gradient is established around chromosomes during mouse meiotic maturation

A RanGTP gradient has been demonstrated to surround the chromatin in *X. laevis* egg extracts and mitotic cells (Kalab et al., 2002, 2006; Caudron et al., 2005). We used a mouse system to determine whether a RanGTP gradient was present in large living cells, for example, the mouse oocyte (∼100 μm in diameter). For this purpose, we used the previously described FRET probe, Rango, which has a high FRET signal when it is liberated from importin β by RanGTP (Kalab et al., 2006). An increase in the FRET signal (increase in I_{FRET}/I_{CFP} ratio) emitted by the

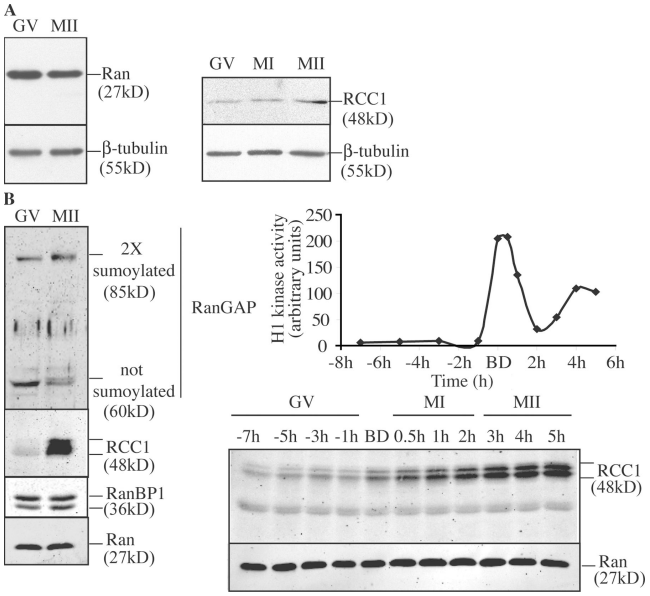

Figure 2. **Characterization of Ran and its regulators in mouse and *X. laevis* oocytes.** (A, left) The amount of Ran protein is stable during meiotic maturation of mouse oocytes. 30 immature (GV) or mature (MII) mouse oocytes were collected and immunoblotted using a monoclonal anti-Ran antibody and an anti-tubulin antibody. (right) The amount of RCC1 increases slightly during meiotic maturation of mouse oocytes. 100 immature (GV), 4 h after GVBD (MI), or mature (MII) mouse oocytes were collected and immunoblotted using a polyclonal anti-RCC1 antibody and an anti-tubulin antibody. (B, left) RCC1 levels increase during meiosis in *X. laevis* oocytes, but RanGAP, RanBP1, and Ran levels remain constant. Oocyte lysates (GV) or egg lysates (MII) were immunoblotted using anti-RanGAP, anti-RCC1, anti-RanBP1, and anti-Ran antibodies. (top right) Histone H1 kinase activity (arbitrary units) during meiotic maturation induced by progesterone. (bottom right) Increase of RCC1 amount during meiosis resumption in *X. laevis*. Two oocytes were used for each time point.

Rango probe indirectly reports RanGTP levels: the presence of a free cargo gradient is indicative of a RanGTP gradient.

The local increase in the I_{FRET}/I_{CFP} ratio (Fig. 3, A and B) indicated the accumulation of free Rango and, hence, RanGTP near the chromosomes. The I_{YFP}/I_{CFP} ratio was consistently high in the same region, confirming the increase in FRET (unpublished data). The distribution of the RanGTP gradient in oocytes shows that RanGTP accumulated around chromosomes and decreased linearly with distance from the metaphase plate (Fig. 3 C). Thus, there was a broad (the size of an oocyte, ∼100 μm), shallow RanGTP gradient in mouse oocytes. We followed RanGTP-induced release of importin β in live oocytes and indirectly detected the accumulation of RanGTP around chromosomes during all steps of mouse meiotic maturation (Fig. 3 D). The kymograph shows that the local accumulation of RanGTP strictly followed the movement of chromosomes to the cortex during MI (Fig. 3 D). This is the first evidence of such a RanGTP gradient occurring during the time course of division in a living organism.

MI spindles that assemble in the presence of low and high levels of RanGTP are functional

We showed that Ran and RCC1 were present in mouse oocytes and that a broad gradient of RanGTP-induced release of importin

β occurred during meiosis resumption. Next, we examined the role of Ran. For this purpose, we manipulated the levels of RanGTP by injecting two mutant forms of Ran into GV-stage oocytes. Ran^{T24N} has much weaker affinity for guanine nucleotide than does wild-type Ran, binds RCC1, and is a potent inhibitor of Ran's GDP–GTP exchange activity (Dasso et al., 1994). Thus, it inhibits the generation of RanGTP. Ran^{Q69L} is unable to hydrolyze GTP and remains locked in the GTP-bound state (Bischoff et al., 1994).

We first checked that our mutants were expressed continuously and at similar levels during mouse meiotic maturation (Fig. S1, A, B, and C, available at http://www.jcb.org/cgi/content/full/jcb.200605199/DC1). We directly measured the efficiency of our mutants in ovo during meiotic maturation by injecting the Rango probe with each mutant form of Ran. The mutants blocked nuclear import in GV oocytes (Fig. 3 E), as described previously (Palacios et al., 1996). From GV to MII, there were lower levels of liberated Rango in oocytes receiving Ran^{T24N} than in controls, consistent with inhibition of RanGTP production (Fig. 3 E, compare 2 and 5 with 1 and 4). There were substantially higher levels of RanGTP in the cytoplasm of oocytes receiving Ran^{Q69L} than in controls (Fig. 3 E, compare 3 and 6 with 1 and 4). In both cases, there was no detectable gradient of RanGTP in oocytes.

We then injected RNA encoding tubulin-GFP with each form of Ran into mouse oocytes and followed spindle formation by video microscopy and by visualization of immunofluorescence after oocyte fixation. Meiosis resumption and first polar body extrusion had similar kinetics in control and injected oocytes (Table I). This suggests that ectopic expression of the different forms of Ran did not affect the cell cycle per se. We observed the same succession of events with kinetics similar to those present in tubulin-GFP–injected oocytes (Fig. 1) in oocytes injected with wild-type Ran (Ran^{WT}; Fig. 4 A and Video 1, available at http://www.jcb.org/cgi/content/full/jcb.200605199/DC1). This shows that overexpression of Ran^{WT} did not affect meiotic

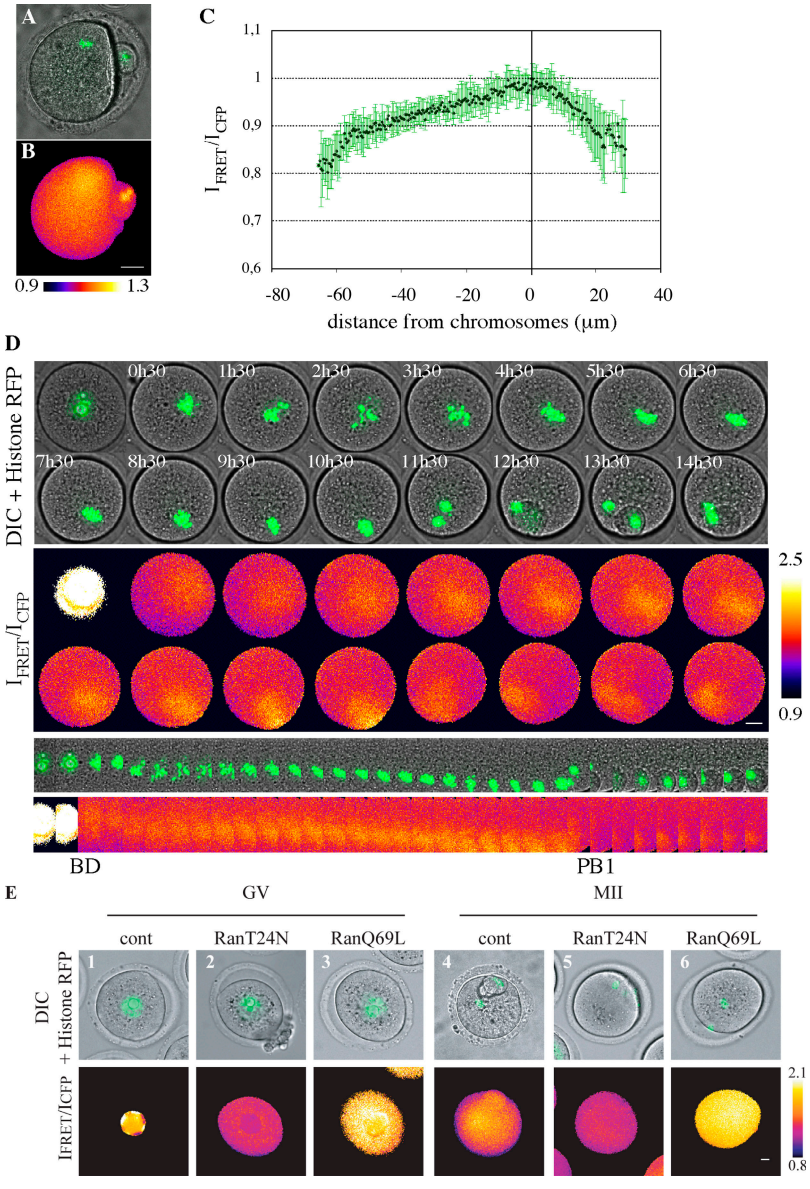

Figure 3. **Detection of a gradient of RanGTP-induced release of importin β in live mouse oocytes.** (A and B) Live MII-arrested mouse oocyte injected with Rango and histone-RFP encoding RNA. (A) Image of phase contrast (DIC) merged with the image of the chromosomes (in green). (B) Pseudocolored I_{FRET}/I_{CFP} ratio of the same oocyte expressing Rango. (C) I_{FRET}/I_{CFP} ratio line scans performed perpendicularly to the metaphase plate from 10 MII oocytes, where the position of the chromosomes was arbitrarily set at 0. (D) Time-lapse microscopy of mouse oocytes injected with histone-RFP and Rango encoding RNA. The top panel corresponds to the phase contrast (DIC) merged with the image of the chromosomes (in green). The bottom panel corresponds to the pseudocolored I_{FRET}/I_{CFP} ratio emitted by the Rango probe. Time after GVBD is indicated in the top left corner on the DIC time-lapse image. The two bottom panels correspond to the kymograph of a cropped region containing the chromosomes from the same time lapse (one image per 30 min) plotted against time. $n = 27$. BD, GVBD; PB1, first polar body extrusion. (E) The gradient of RanGTP-regulated release of importin β is perturbed by Ran^{T24N} or Ran^{Q69L} throughout meiotic maturation. Immature (GV; 1, 2, and 3) or metaphase II–arrested (MII; 4, 5, and 6) mouse oocytes injected with Rango and histone-RFP encoding RNA alone (1 and 4; $n = 30$) or further injected either with Ran^{T24N} (2 and 5; $n = 41$ for GV and 37 for MII) or Ran^{Q69L} (3 and 6; $n = 43$ for GV and 36 for MII). (top) Image of phase contrast (DIC) merged with the image of the chromosomes (in green); (bottom) pseudocolored I_{FRET}/I_{CFP} ratio of the corresponding oocyte expressing Rango. The same scale of colors was applied to all samples. Bars, 20 μm.

maturation and spindle assembly, which is consistent with a previous report (Moore et al., 2002).

Asters appeared in the cytoplasm after GVBD, not exclusively around the chromosomes in mouse oocytes injected with Ran^{Q69L}, consistent with observations made in *X. laevis* egg extracts. These asters fused to form a bipolar spindle that was abnormally long (Fig. 4 B; Fig. 5, A and B; and Videos 2 and 3, available at http://www.jcb.org/cgi/content/full/jcb.200605199/DC1). 7 h after GVBD, spindles with a similar size as those in control oocytes (47% were within the range of the standard deviation for control spindles) or longer (averaging 30% longer) were present in 53% of the oocytes (Fig. 5, A, B, and C). The MI spindle that formed under these conditions migrated, and the pole closest to the cortex pushed into the cortex. Consistent with the formation of longer spindles in oocytes injected with Ran^{Q69L}, 58% of the oocytes extruded a large first polar body (Table I).

Ran^{T24N} injected into mouse oocytes delayed the establishment of MI spindle bipolarity by ~3 h in most oocytes (Fig. 4 C; Fig. 5, A, B, and C; and Video 4, available at http://www.jcb.org/cgi/content/full/jcb.200605199/DC1). During this time, MTs were unorganized around the chromosomes (Fig. 5, A, B, and C). Approximately 5 h after GVBD, two poles formed and a spindle with very small poles assembled around chromosomes. Despite a 3-h delay in spindle formation, anaphase took place normally and the first polar body was extruded.

Direct control of MTOC distribution by Ran GTPase did not cause the observed defects in MI spindle formation after overexpression of Ran variants. Oocytes injected with either mutant form of Ran had γ-tubulin foci randomly distributed

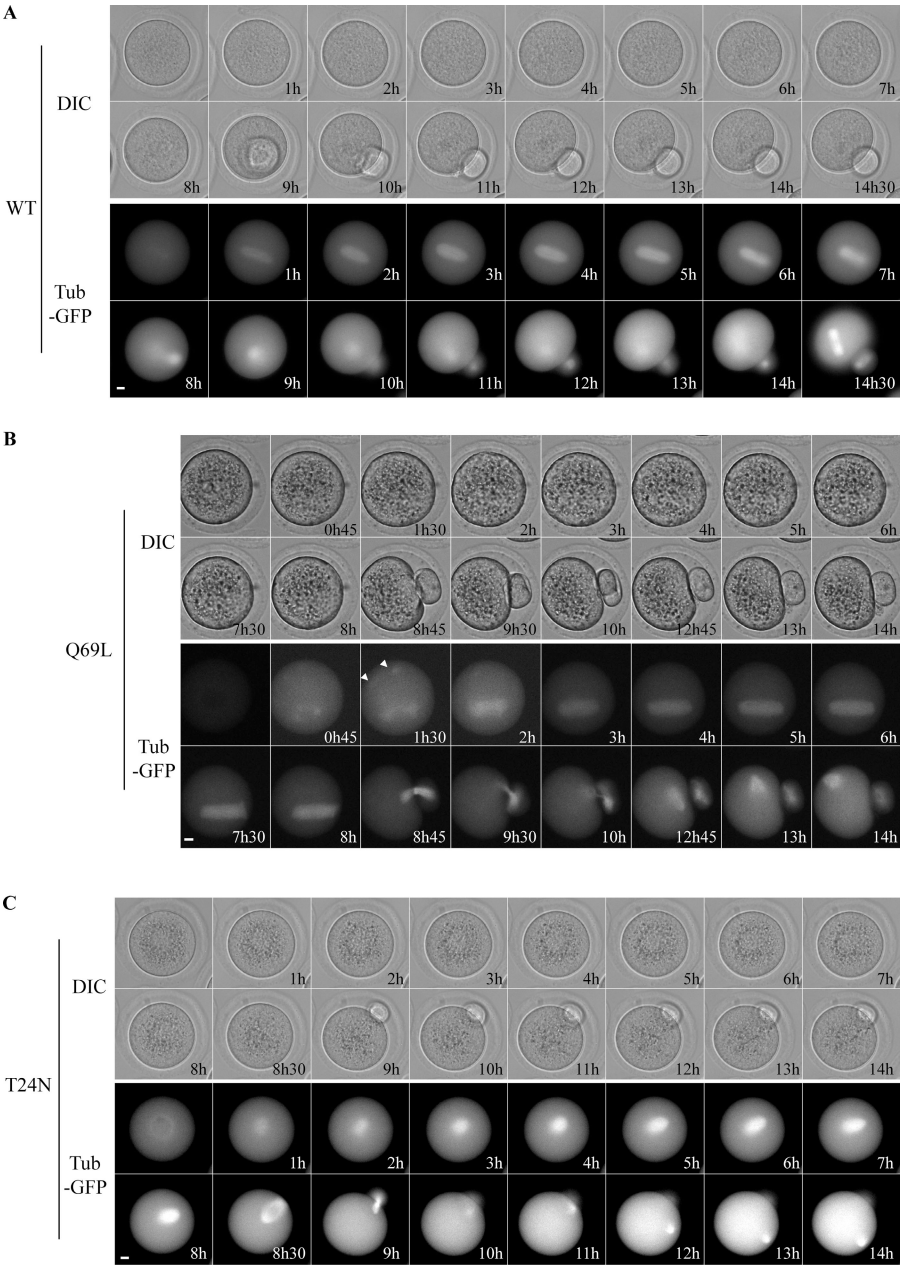

Figure 4. **Excess or reduced levels of RanGTP induce spindle defects during meiosis I and II of mouse oocytes.** Time-lapse microscopy of phase contrast (DIC) and tubulin-GFP (Tub-GFP) of oocytes injected with tubulin-GFP together with Ran^{WT} (A) or Ran^{Q69L} (B) or Ran^{T24N} (C) RNA. Images were taken every 15 min. Arrowheads indicate asters. Times after GVBD are indicated in the bottom right corner. n = 34 (Ran^{WT}), 26 (Ran^{Q69L}), and 75 (Ran^{T24N}). Bars, 10 μm.

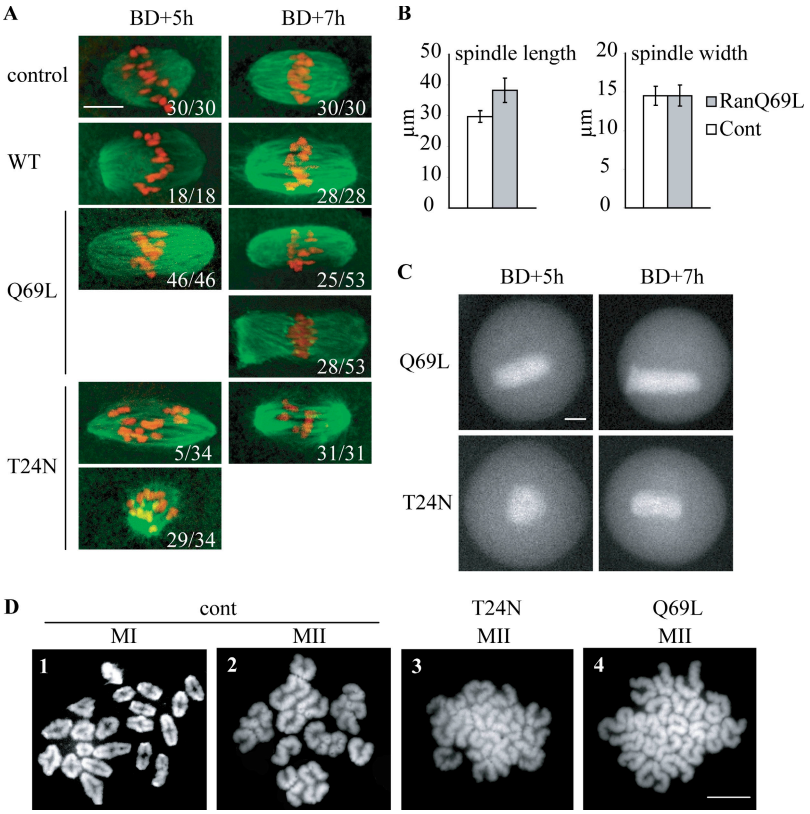

Figure 5. **MI spindle defects induced by excess or reduced levels of RanGTP do not compromise homologous chromosome segregation.** (A and B) Ran^{Q69L}-injected oocytes assemble longer spindles with poles defects, whereas Ran^{T24N} induces a lack of MT assembly associated with a delay in spindle formation. (A) Immature oocytes were microinjected with Ran^{WT}, Ran^{Q69}, or Ran^{T24N}, collected 5 or 7 h after GVBD and immunostained for MTs (green) and DNA (red). Oocytes were analyzed by confocal microscopy, and all confocal sections were projected. Proportions of each phenotype are indicated in the bottom right corner. (B) Statistics of spindle length and width in control and Ran^{Q69L}-injected oocytes. Error bars indicate SD. (C) Still images taken from time-lapse microscopy of tubulin-GFP (Tub-GFP) of oocytes injected with tubulin-GFP together with Ran^{Q69L} or Ran^{T24N} RNA. (D) Meiosis I spindles assembled with modified RanGTP levels can segregate homologous chromosomes. Noninjected control oocytes were collected 6 h (MI) or 12 h (MII) after GVBD and submitted to chromosome spread preparation. MI preparation shows only bivalent chromosomes with chiasmata, whereas MII preparation shows only univalent chromosomes (1 and 2). Ran^{T24N}- or Ran^{Q69L}-injected oocytes were collected 12 h after GVBD (MII) and similarly submitted to chromosome spread preparation (3 and 4). In both cases, only univalent chromosomes are seen. 25 oocytes were analyzed for each condition. Bars, 10 µm.

around condensing chromosomes 1 h after GVBD, as in controls (Fig. S1 E). The distribution of γ-tubulin foci in oocytes injected with Ran mutants was different from the distribution in controls because it is MT dependent (Fig. S1 E, cont + Noco).

We analyzed chromosome spreads from control and injected oocytes that had undergone MI to assess whether meiosis I spindles that formed in the presence of Ran^{Q69L} or Ran^{T24N} were functional. MII-arrested oocytes had only 20 monovalent chromosomes in all cases (Fig. 5 D, compare 2, 3, and 4), showing that homologous chromosome segregation occurred normally.

The Ran pathway is essential for meiosis II

MII spindles formed after Ran^{Q69L} and Ran^{T24N} expression in mouse oocytes were much more disorganized than MI spindles under these conditions (Fig. 4, B and C). The injection of Ran^{WT} did not affect MII spindle organization (Fig. 4 A and Fig. 6, A [2] and B), as observed by live imaging. The injection of Ran^{Q69L} and Ran^{T24N} induced similar spindle defects in MII. Oocytes either displayed an opened bipolar spindle connected to numerous cytoplasmic asters (50% of oocytes injected with Ran^{Q69L} and 78% of Ran^{T24N}; Fig. 6, A [3 and 4] and B) or no organized spindle (30% of oocytes injected with Ran^{Q69L} and 17% of oocytes injected with of Ran^{T24N}; Fig. 6, A [5 and 6] and B). The expression levels of our constructs were very similar in oocytes injected with Ran^{WT}, Ran^{Q69L}, and Ran^{T24N} (Fig. S1 D).

We activated MII oocytes that had been injected with Ran^{WT} and Ran^{T24N} with strontium, as described previously (Tsurumi et al., 2004) to determine whether spindles assembled in the presence of Ran mutants were functional. Controls (noninjected or Ran^{WT}-injected oocytes) and Ran^{T24N}-injected oocytes had similar levels of activation (Table II). Nevertheless, MII to anaphase II transition was much slower (with a 2-h delay) in oocytes injected with Ran^{T24N} than in controls. This suggests that the spindle checkpoint was activated in these oocytes, potentially slowing the exit from CSF arrest. This observation is consistent with the observed MII spindle defects after injection of Ran^{T24N}. Furthermore, all oocytes injected with Ran^{T24N} had severe cytokinesis defects: they cleaved instead of extruding a second polar body (Table II and Fig. 6 C), and membrane blebbing was often present in the cytokinetic furrow. We observed obvious segregation defects in 46% of these oocytes but did not see these defects in controls. Only one pronucleus was present in control oocytes, whereas there were lagging chromosomes in Ran^{T24N}-injected oocytes (Table II and Fig. 6 C). Thus, overexpression of Ran^{T24N} strongly impaired the progression of meiosis II.

The role of Ran in meiotic spindle assembly in *X. laevis* oocytes

Our findings in mouse oocytes suggest that inhibition of RanGTP production primarily perturbed spindle formation during meiosis II without completely inhibiting the establishment of meiosis I spindles and without affecting entry into the M phase. As shown in Fig. 2, RCC1 levels in immature and mature oocytes were very different in *X. laevis* oocytes. Increasing RCC1 levels in *X. laevis* oocytes throughout meiotic maturation suggest that RanGTP has an important function during MII. As RCC1 levels rise substantially during maturation of oocytes, preventing the synthesis of RCC1 during maturation kept RCC1 levels lower than in controls. Injection of antisense

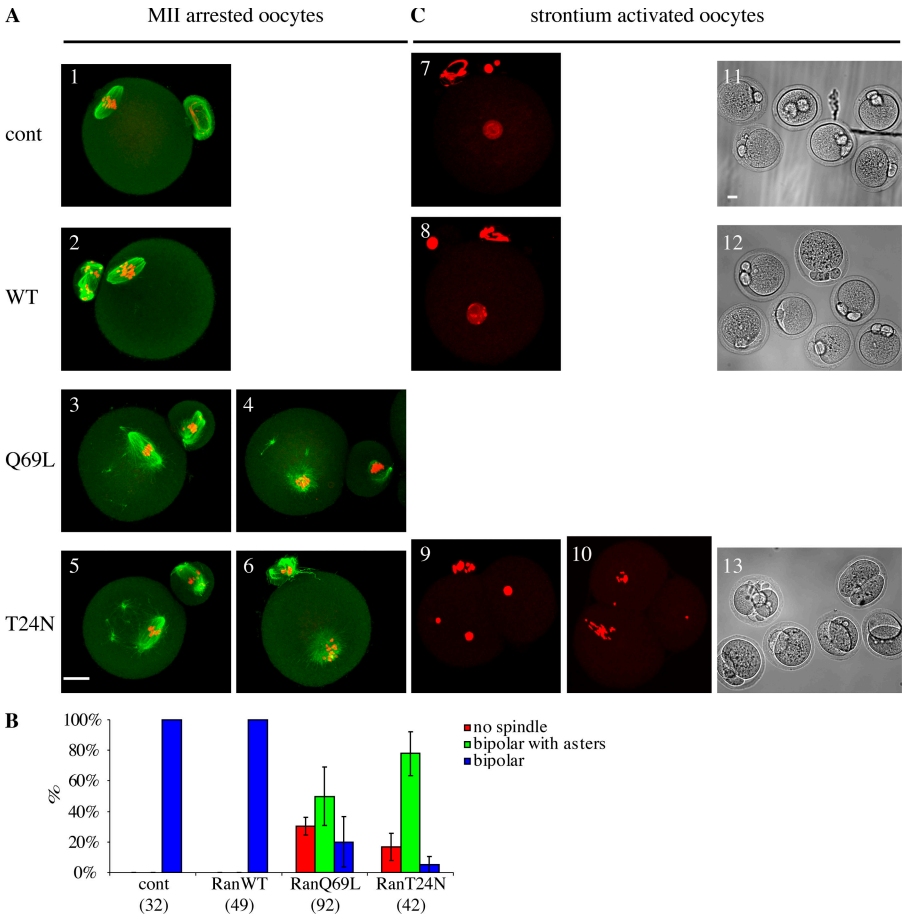

Figure 6. **Spindle defects induced by excess or reduced levels of RanGTP during meiosis II.** (A) MII oocytes collected 15 h after GVBD and immunostained for MTs (green) and DNA (red). (1) Control noninjected oocyte; (2–6) immature oocytes were microinjected with Ran^{WT} (2), Ran^{Q69L} (3 and 4), or Ran^{T24N} (5 and 6). Oocytes were analyzed by confocal microscopy, and all confocal sections were projected. Bar, 20 μm. (B) Statistics of the experiment described above. "No spindle" indicates oocytes showing monopolar structure or a single aster around chromosomes with or without numerous asters in the cytoplasm. "Bipolar with asters" indicates oocytes showing an opened bipolar structure around chromosomes connected to numerous asters in the cytoplasm, and "bipolar" indicates oocytes showing a normal bipolar MII spindle. The number in parentheses corresponds to the total number of oocytes analyzed. Error bars indicate SD. (C) MII-arrested oocytes were activated with strontium to allow the metaphase II–anaphase II transition. Oocytes were observed 5 h after Sr2+ activation either after chromosome labeling to visualize the pronuclei (7–10) or by transmitted light to visualize the second polar bodies (11–13). Ran^{T24N}-injected oocytes presented a 2-h delay in their progression to interphase as indicated by the retarded decondensation of chromatin in these oocytes compared with controls. Immature oocytes were either noninjected (7 and 11) or microinjected with Ran^{WT} (8 and 12) or Ran^{T24N} (9, 10, and 13) and then activated after their arrest in MII and observed 5 h after activation.

deoxyoligonucleotides prevented the rise in RCC1 levels, which occurs concomitantly with meiosis resumption (Fig. 7, A and C). The knock down of RCC1 did not modify the kinetics of meiosis resumption (not depicted) and meiosis I spindle formation (Fig. 7, D and E). In control and RCC1 knockdown samples, 75–90% of MI spindle structures looked normal (Fig. 7 E). Similar to our findings in mice, oocytes with low levels of RCC1 and, thus, low levels of RanGTP, progressed through MI, as observed by polar body extrusion (not depicted) and the drop in histone H1 kinase activity after GVBD in both control and RCC1-depleted oocytes (Fig. 7 B).

Similar to meiosis in mouse oocytes, MII spindle formation was sensitive to perturbation of the GTP–GDP cycle of Ran. Although 67% of the spindles in sham-injected *X. laevis* oocytes had normal bipolar organization and aligned chromosomes (76% in uninjected controls), only 14% looked normal after RCC1 knockdown, and 86% of the structures were aberrant (monopolar MT structures, spindle-like structures without a correct antiparallel array of MTs around the chromosomes and without chromosome alignment) or appeared as chromatin aggregates with no MTs (Fig. 7, F and G). These spindle defects were not caused by disruption of Cdk1 activities, as shown by histone H1 kinase assays (Fig. 7 B).

Our findings suggest that *X. laevis* oocyte maturation requires a large increase in RCC1 levels and, thus, RanGTP production. Inhibition of RCC1 activity led to defects in MII, as in mice. Thus, the mechanisms of meiotic spindle assembly in mice and *X. laevis* have similar principles: local RanGTP production is essential during MII but much more weakly influences spindle function during the reductive first meiotic cell division.

Discussion

In this study, we investigated the function of Ran during assembly of the first and second meiotic spindles in living mouse and *X. laevis* oocytes, two vertebrate models of acentrosomal spindle formation. We microinjected Ran mutants and directly monitored RanGTP levels by FRET in mouse oocytes, or we knocked down RCC1 in *X. laevis*. Ran regulated meiosis I spindle formation differently than meiosis II spindle formation in these two models.

Evidence for a broad RanGTP-regulated gradient

We are confident that the FRET probe we used for the indirect detection of the RanGTP-regulated gradient functions normally in our model system for two reasons. First, the probe behaved as expected in GV oocytes. It was imported as a cargo into the nucleus. Also, its FRET emission was highest where RanGTP-induced release of importin β and, therefore, RanGTP concentration should have been highest, i.e., in the GV (Kalab et al., 2002, 2006). Second, the Rango probe responded as expected to overexpression of the two well-characterized Ran mutants

Table II. **Percentage of activation, cleavage, and obvious chromosome missegregation after activation of MII oocytes by strontium**

Type of oocyte	PB2	Large PB2	Obvious missegregations
	%	%	%
Control (n = 53)	96.2	0	0
Wild type (n = 29)	79.3	0	0
T24N (n = 32)	81.2	100	46.2

Percentage of second polar body extrusion (PB2). Percentage of abnormally large second polar body estimated visually (large PB2). Percentage of obvious missegregation after activation (more than one pronucleus in one cell, lagging chromosomes).

(Fig. 3 E). The analysis of the distribution of RanGTP in oocytes showed that it accumulated around chromosomes and decreased linearly with distance from the metaphase plate. This suggests that the gradient of RanGTP in mouse oocytes was shallower than that observed in *X. laevis* egg extracts and HeLa cells (Kalab et al., 2002, 2006). It resembles to some extent the broad gradient observed by Caudron et al. (2005). We also followed changes in the gradient in real time. We consistently observed a huge drop in RanGTP levels relative to the GV content at the periphery of MI chromatin immediately after GVBD. The drop in free Rango concentration (corresponding with RanGTP levels) suggests that meiotic cytoplasm contains relatively higher levels of RanGAP activity than cytoplasm in mitotic HeLa cells (Kalab et al., 2002), resulting in low overall levels of RanGTP. Despite the substantial drop in the free Rango concentration around the chromatin, the chromosomes remained surrounded by a localized gradient of free importin β cargos throughout MI and MII. This appears to be particularly important in maturing mammalian oocytes, in which chromosomes migrate to the cortex before cytokinesis in MI (Verlhac et al., 2000a). The positional information given by local RanGTP accumulation and carried during chromosome migration in MI might be important for the asymmetry of the division. The cleavage phenotype observed in Ran^{T24N}-injected oocytes undergoing parthenogenetic activation suggests that local accumulation of RanGTP is essential for the asymmetry of the second meiotic division.

Ran mediates spindle length and timing of bipolarity establishment but not recruitment of MTOCs in meiosis I

The Ran protein level was constant throughout meiotic maturation in *X. laevis* and mouse oocytes. If we overexpressed wild-type Ran during MI in mouse oocytes, meiosis I was not altered and the spindle assembled normally. This indicates that it is not the overall level of Ran that is important but the concentration of RanGTP. If we expressed Ran^{Q69L} during mouse MI, ectopic asters assembled in the cytoplasm and were rapidly incorporated into the forming spindle. Thus, in vivo, if active Ran was ectopically expressed in the cytoplasm, spindle formation occurred despite the promotion of ectopic aster assembly. This finding is consistent with previously described effects of the Ran^{Q69L} mutant on spindle formation in *X. laevis* egg extracts (Carazo-Salas et al., 2001). The mechanism of aster incorporation into the spindle is unknown but could be associated with

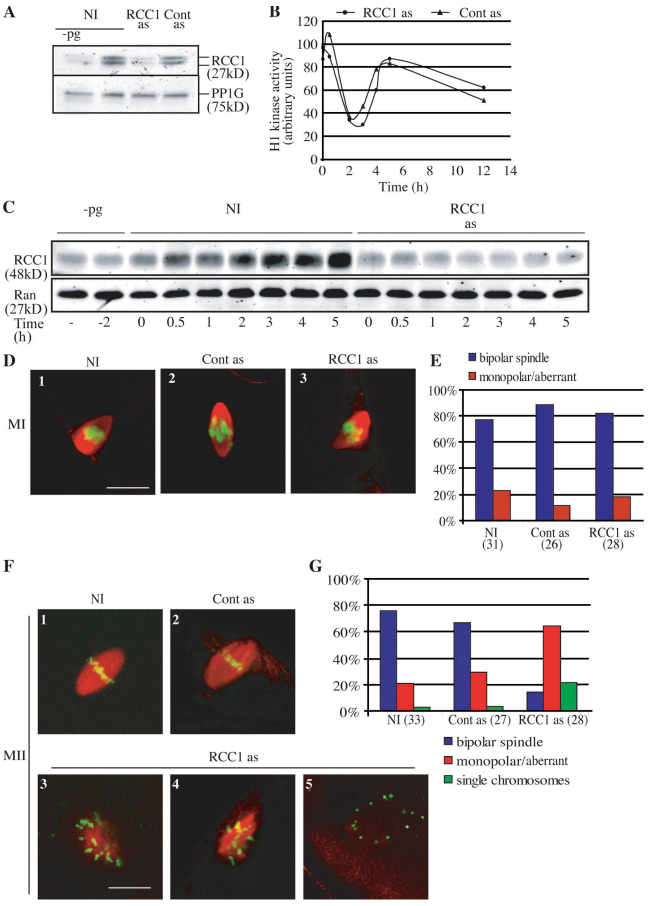

Figure 7. **Down-regulation of RCC1 during meiotic maturation in *X. laevis* oocytes does not compromise meiosis I spindle formation but affects the meiosis II spindle.** (A) Western blot on oocyte lysates using antibodies against RCC1 or PP1G as loading control, before (−pg) and 12 h after induction of maturation with progesterone in nontreated (NI), control injected (Cont as), or RCC1 knockdown (RCC1 as) samples. (B) Histone H1 kinase activities were measured with time after GVBD in control injected (triangles) and RCC1 knockdown (circles) oocytes. (C) Western blot on oocyte lysates using antibodies against RCC1 and Ran as loading control, before and after induction of maturation with progesterone in nontreated controls or antisense RCC1-injected oocytes. Samples were taken before progesterone addition or after GVBD (GVBD corresponds to time 0). (D–G) Representative images (D and F) and quantitative analysis of imaged structures (E and G) of spindles visualized in MI (D and E; 1.5 h after GVBD) or MII (F and G; 12 h after GVBD) by indirect immunofluorescence with antibodies against α-tubulin (red) or Cytox green (green) of oocytes treated as in (A, B, and C). Bars, 20 μm.

the capacity of MTs to "self-organize" and assemble into bipolar spindles (Karsenti and Vernos, 2001). After MI, 53% of the spindles formed in the presence of Ran^{Q69L} were considerably longer (30% longer) than those found in control oocytes. Recently, it was shown in *D. melanogaster* S2 cells that the length of the spindle is sensitive to alterations in MT dynamics (Goshima et al., 2005). We hypothesize that Ran^{Q69L} expression leads to an increase in MT stabilization and, thus, to lengthening of the spindle. As the central spindle defines the position of the cleavage furrow and the MI spindle is perpendicular to the oocyte cortex, a longer spindle should give a more symmetric division. We observed that 58% of Ran^{Q69L}-injected oocytes extruded a much larger polar body than controls.

Despite the early ectopic asters and long length, all MI spindles in Ran^{Q69L}-injected mouse oocytes that we analyzed had normal chromosome segregation. Therefore, the increase in RanGTP did not compromise homologous chromosome segregation but did compromise the asymmetry of the first division in ~50% of the oocytes. This asymmetry is essential for the preservation of maternal stores for the future embryo. Thus, it is important for the gamete to regulate its RanGTP levels to remain fertile.

Ran^{T24N} expression during MI induced a delay in spindle bipolarity establishment of ~2–3 h. This could be explained by low MT assembly activity in these oocytes, consistent with findings from *X. laevis* egg extracts. During MI in mouse oocytes, spindle poles are defined by the distribution of MTOCs, which aggregate progressively at the two opposite poles of the forming spindle. This distribution seems to be dependent on MTs, which we demonstrate assemble at low RanGTP levels. We hypothesize that if MT assembly is inefficient, it is difficult to distribute MTOCs and to establish two poles. However, despite substantially low RanGTP production because of Ran^{T24N} expression, a functional bipolar spindle can assemble in time. Similar principles are probably in place in *X. laevis*, because RCC1 levels continuously increased during meiotic maturation. Thus, levels of RCC1 are lower in MI than in MII. This is consistent with RanGTP production having an important function during MII in *X. laevis*. Inhibition of RCC1 expression did not prevent MI spindle assembly or extrusion of the first polar body but led to large defects only during MII in *X. laevis* oocytes. Although the decrease in RCC1 levels after injection of antisense oligos was smaller in MI than in MII, MI occurred in the presence of the same absolute levels of RCC1. However, these levels were insufficient for MII. Thus, our findings suggest that there are similar principles controlling meiotic spindle assembly in mice and *X. laevis*: local RanGTP production is crucial during MII but is less important during MI.

Our findings indicate that in mouse oocyte meiosis I, the Ran pathway controls spindle length and the timing of bipolarity establishment. However, pathways acting in parallel can compensate for defects induced by disruption of Ran function, even in the absence of centrosomes, which is characteristic of this system.

RanGTP is essential for spindle formation and correct progression in meiosis II

Ran^{Q69L} is locked in the GTP-bound form and, thus, constitutively activates its targets. If active Ran was ectopically expressed in mouse oocytes by Ran^{Q69L} expression, Ran targets were probably activated in the cytoplasm and not only around chromosomes. These compete for additional MT assembly factors and uncouple MT formation from chromosomes. We obtained unexpected results with Ran^{T24N} expression during MII. This mutant has been shown to inhibit spindle assembly in *X. laevis* egg extracts (Carazo-Salas et al., 1999; Kalab et al., 1999; Ohba et al., 1999; Wilde and Zheng, 1999). Expressing this mutant during MII in mouse oocytes led to defects very similar to those obtained with Ran^{Q69L}. At this point, we can only speculate how manipulating RanGTP levels induces apparently identical phenotypes with multiple ectopic asters in MII oocytes. Possibly, RanGTP activates a spindle-stabilizing factor specific to MII and its activation by Ran^{Q69L} induces ectopic MT assembly. In Ran^{T24N}-injected oocytes, this factor would not be activated and the spindle would no longer be stabilized. Spindle fragmentation may lead to the formation of ectopic structures.

Although metaphase is a transient state of MI or mitosis, it can last for many hours or even days (until fertilization occurs) in MII-arrested oocytes. This suggests that alternative mechanisms to those present in systems that have been used for analysis of mitotic Ran function are acting in the mouse meiosis II model. We have shown previously that MII spindle organization must be maintained by meiosis II–specific mechanisms, which involve at least two proteins, MISS (MAPK-interacting and spindle stabilizing) and DOC1R (deleted in oral cancer 1 related; Lefebvre et al., 2002; Terret et al., 2003). The depletion of MISS in mouse oocytes leads to phenotypes that resemble that observed in Ran^{T24N}-expressing MII oocytes. We are now testing the hypothesis that MISS may in fact act as a RanGTP-regulated spindle-stabilizing factor.

In this study, we show that manipulating RanGTP levels in mouse oocytes (with the injection of the Ran^{T24N} mutant) strongly compromises the fidelity of sister chromatid segregation and the asymmetry of the second meiotic division. We did not observe obvious defects after manipulation of RanGTP levels in meiosis I similar to those observed in meiosis II. This strongly suggests that meiosis II spindle assembly is more sensitive to changes in the RanGTP gradient than meiosis I.

Different mechanisms for meiosis I and II spindle formation

In mouse oocytes, the first meiotic M phase is very long, lasting from 6 to 11 h, depending on the genetic background (Polanski, 1986, 1997). In *X. laevis* oocytes, the first meiotic spindle also assembles progressively from a large monopolar aster (Gard, 1992). In these two models, the second meiotic M phase is also very long, lasting hours or even days until fertilization occurs. However, the MII spindle assembles rapidly, and 1 h after the first polar body emission in mouse oocytes a stable bipolar spindle has already formed. It has been reported recently that during mitosis, the classical search-and-capture mechanism is not fast enough to account for observed rates of spindle assembly (Wollman et al., 2005). The RanGTP gradient around chromosomes would introduce a bias, improving the efficiency of search-and-capture and speeding up spindle assembly. However, we speculate that, even if the gradient is present in mouse oocytes, this bias is not required when the M phase lasts several hours, as is the case in MI. MII spindle formation in *X. laevis* oocytes is faster than MI spindle formation (Gard, 1992). This may explain why the Ran pathway mediates the timing of bipolarity establishment during MI in mouse and in *X. laevis* but is dispensable for the formation of a functional bipolar spindle. Consistent with this, when the spindle forms rapidly during MII, the presence of a RanGTP gradient around chromosomes is necessary for the establishment of a bipolar spindle.

Materials and methods

Mouse oocyte collection, culture, and microinjection

Oocytes were collected from 11-wk-old OF1 female mice, cultured, and microinjected as described previously (Verlhac et al., 2000b). Oocytes were maintained at the GV stage in M2 medium supplemented with 50 μg/ml dbcAMP (Sigma-Aldrich; Whittingham, 1971). In vitro synthesized RNAs were microinjected into the cytoplasm of GV oocytes. Injected oocytes were kept in M2 + BSA medium supplemented with dbcAMP for 3 h to allow overexpression of the corresponding protein. The resumption of meiotic maturation (GVBD) was triggered upon release of the oocytes into a drug-free medium. MII oocytes were released from CSF arrest using 10 mM strontium in Ca^{2+}/free M2 medium as described by Tsurumi et al. (2004).

In vitro maturation of *X. laevis* oocytes

Collagenase-treated stage VI oocytes were incubated in 5 μg/ml progesterone (Sigma-Aldrich) containing Barth buffer. Oocytes were checked every 10 min for GVBD spot appearance. Oocytes with appearing GVBD spots were collected and further incubated for the indicated times. Oocytes used for immunoblotting and H1-kinase assay were frozen in liquid nitrogen and for immunofluorescence staining fixed in 20% DMSO and 80% methanol.

Plasmid construction and in vitro transcription of synthetic RNA

pQE32-cRan, pQE32-hRan^{Q69L}, and pQE32-hRan^{T24N} were a gift from D. Görlich (Zentrum für Molekulare Biologie der Universität Heidelberg, Heidelberg, Germany). The coding sequences of canine Ran and human Ran^{Q69L} and Ran^{T24N} were subcloned by PCR at EcoRI–NotI sites of the pRN3-myc2 vector. The pRN3-β5-tubulin-GFP plasmid has been described (Brunet et al., 1998). The Rango probe was subcloned into pRN3. The pRN3-histone RFP has been described (Tsurumi et al., 2004). The in vitro synthesis of capped RNA was performed as described previously (Terret et al., 2003).

Videomicroscopy

Hoechst live, tubulin-GFP, histone-RFP, and Rango emission were visualized using a PL Fluotar 20×/0.5 objective lenses or a HC PL APO 20×/0.7 NA objective lenses (Leica) and a charge-coupled device camera (Micromax; Roper Scientific) under a computer-controlled videomicroscope (DM IRBE; Leica) enclosed in a thermostatic chamber (Life Imaging Services). For the FRET, exposure times were 100 ms. The fluorescence images were collected through 440AF21 excitation filter, 455 dichroic mirror, 480AF30 emission filter for CFP, and 535AF26 emission filter for FRET. The RFP images were obtained through a 546 ± 6 excitation filter, a 565 dichroic mirror, and a 620 ± 20 emission filter.

MetaMorph 7.0 (Universal Imaging) and ImageJ (NIH) were used for image analysis. The pixel alignment of the CFP, FRET, and RFP images was verified and adjusted. Background values were calculated within a region of interest outside the cell. Ratios were calculated after background subtraction by pixel-wise divisions of the images in the CFP and FRET channels.

Immunofluorescence

Immunofluorescence of mouse oocytes was performed as described previously (Brunet et al., 1999). For MTs, we used a rat monoclonal antibody against tyrosinated α-tubulin (YL1/2). γ-Tubulin was visualized using a rabbit polyclonal anti–γ-tubulin antibody (1:1,000; Abcam). Samples were observed with a confocal microscope (TCS-SP; Leica) using a Plan APO 40×/1.25. Z series were performed with one image per micrometer, and a maximum projection of all Z planes is shown.

X. laevis oocytes were processed essentially as described previously (Schwab et al., 2001). In detail, DMSO/methanol permeabilized oocytes were fixed in methanol overnight at –20°C, rehydrated in PBS, and blocked with 5% BSA in PBS. Oocytes were then incubated with monoclonal anti–α-tubulin antibody (Clone DM 1A; Sigma-Aldrich), washed, and incubated with Cy3-labeled goat anti–mouse antibody (Jackson ImmunoResearch Laboratories). Oocytes were washed again with PBS, transferred into 0.5× TBS buffer (12.5 mM Tris, pH 7.2, and 60 mM NaCl), incubated with 5 μM Cytox green (Invitrogen), and washed with 0.5× TBS. Oocytes were dehydrated in methanol again and transferred into Murray's solution (benzylalcohole/benzylbenzoate, 1:2). After clarification, oocytes were cut within the GVBD spot and placed on depression microscope slides. Images were taken using a confocal microscope (TCS-NT; Leica).

Immunoblotting

Immunoblotting of mouse oocytes was performed as described previously (Terret et al., 2003). *X. laevis* oocytes were lyzed in H1 kinase buffer and centrifuged at 12,000 *g* for 15 min. Amounts corresponding to two thirds of the total lysate of one oocyte were used for immunoblotting. The supernatant was analyzed by immunoblotting.

Antibodies

For mouse oocytes, Ran was recognized using a monoclonal antibody from BD Biosciences. For *X. laevis* oocytes, rabbit polyclonal anti-human RCC1 and Ran were described previously (Hetzer et al., 2000), polyclonal antibody against RanGAP was a gift from T. Walther and I. Mattaj (European Molecular Biology Laboratory, Heidelberg, Germany), and rabbit polyclonal antibody against RanBP1 was a gift from M. Dasso (National Institutes of Health, Bethesda, MD). A rabbit polyclonal antibody against PP1G was used as control in Fig. 6 A. It was generated using recombinant full-length *X. laevis* PP1G as antigen in accordance with standard procedures. For detection and quantification of secondary antibody signals on Western blots, an Odyssey system (Li-Cor) was used.

Chromosome preparations from mouse oocytes

Chromosome preparations were performed as described previously (Hodges and Hunt, 2002). Chromosomes were stained using 5 μg/ml propidium iodide in distilled water, and slides were mounted in Citifluor (UKC Chemlab).

Histone H1 kinase assay

X. laevis oocyte lysates prepared as described for immunoblotting were incubated with histone H1 (Sigma-Aldrich) and γ-[^{32}P]ATP as described previously (Felix et al., 1989). Amounts corresponding to one third of the total lysate of one oocyte were used for H1 kinase assays.

Antisense experiments

Antisense oligonucleotides were designed against the two most common alleles of RCC1 mRNA found in the *X. laevis* EST database (Sanger Institute). An oligonucleotide pair against RCC1 mRNA regions −18 to +6, CTTTCATAGTGCCGTCTGTTCTACA, and −18 to +7, CTTTTCATAGTGCAGTCTGTTCTCA, was used to inhibit RCC1 expression. As a control, an oligonucleotide pair against RCC1 mRNA region −44 to −20 was used: GATTACAAAATAAACCGCGCTCGCC and GATTACAAAATTAACCGCGCTCAGC, which led only to a very mild reduction of RCC1 levels (RCC1 amount between 80 and 100% of untreated oocytes). 75 ng of an oligo pair in PBS (37.5 ng/oligo) were injected per oocyte before progesterone addition. Efficiency of RCC1 expression inhibition was routinely tested by immunoblotting.

Online supplemental material

Fig. S1 shows that Ran mutants are stably expressed during meiotic maturation. Video 1 shows control mouse oocytes expressing tubulin-GFP together with Ran^{WT} during meiotic maturation. Videos 2 and 3 show mouse oocytes expressing tubulin-GFP together with Ran^{Q69L} during meiotic maturation. Video 4 shows mouse oocytes expressing tubulin-GFP together with Ran^{T24N} during meiotic maturation. Online supplemental material is available at http://www.jcb.org/cgi/content/full/jcb.200605199/DC1.

We thank Richard Schwartzmann from the Service d'Imagerie of the IFR 83. We thank Mary Dasso, Iain Mattaj, Martin Hetzer, and Tobias Walther for antibodies and Dirk Görlich for providing Ran constructs and support.

This work was supported by grants from the Ligue Nationale contre le Cancer (Ligue Label to C. Jessus and M.-H. Verlhac) and from the Agence Nationale pour la Recherche (ANRNT05-1-43120 to M.H. Verlhac). J. Dumont is a recipient of a fellowship from the Ministère délégué à la Recherche et aux Nouvelles Technologies (bourse ACI).

Submitted: 31 May 2006
Accepted: 20 December 2006

References

Askjaer, P., V. Galy, E. Hannak, and I.W. Mattaj. 2002. Ran GTPase cycle and importins alpha and beta are essential for spindle formation and nuclear envelope assembly in living *Caenorhabditis elegans* embryos. *Mol. Biol. Cell.* 13:4355–4370.

Bamba, C., Y. Bobinnec, M. Fukuda, and E. Nishida. 2002. The GTPase Ran regulates chromosome positioning and nuclear envelope assembly in vivo. *Curr. Biol.* 12:503–507.

Bischoff, F.R., C. Klebe, J. Kretschmer, A. Wittinghofer, and H. Ponstingl. 1994. RanGAP1 induces GTPase activity of nuclear Ras-related Ran. *Proc. Natl. Acad. Sci. USA.* 91:2587–2591.

Brunet, S., Z. Polanski, M.H. Verlhac, J.Z. Kubiak, and B. Maro. 1998. Bipolar meiotic spindle formation without chromatin. *Curr. Biol.* 8:1231–1234.

Brunet, S., A.S. Maria, P. Guillaud, D. Dujardin, J.Z. Kubiak, and B. Maro. 1999. Kinetochore fibers are not involved in the formation of the first meiotic spindle in mouse oocytes, but control the exit from the first meiotic M phase. *J. Cell Biol.* 146:1–12.

Carazo-Salas, R.E., G. Guarguaglini, O.J. Gruss, A. Segref, E. Karsenti, and I.W. Mattaj. 1999. Generation of GTP-bound Ran by RCC1 is required for chromatin-induced mitotic spindle formation. *Nature.* 400:178–181.

Carazo-Salas, R.E., O.J. Gruss, I.W. Mattaj, and E. Karsenti. 2001. Ran-GTP coordinates regulation of microtubule nucleation and dynamics during mitotic-spindle assembly. *Nat. Cell Biol.* 3:228–234.

Caudron, M., G. Bunt, P. Bastiaens, and E. Karsenti. 2005. Spatial coordination of spindle assembly by chromosome-mediated signaling gradients. *Science.* 309:1373–1376.

Ciciarello, M., and P. Lavia. 2005. New CRIME plots. Ran and transport factors regulate mitosis. *EMBO Rep.* 6:714–716.

Dasso, M., T. Seki, Y. Azuma, T. Ohba, and T. Nishimoto. 1994. A mutant form of the Ran/TC4 protein disrupts nuclear function in *Xenopus laevis* egg extracts by inhibiting the RCC1 protein, a regulator of chromosome condensation. *EMBO J.* 13:5732–5744.

Felix, M.A., J. Pines, T. Hunt, and E. Karsenti. 1989. A post-ribosomal supernatant from activated *Xenopus* eggs that displays post-translationally regulated oscillation of its $cdc2^{+}$ mitotic kinase activity. *EMBO J.* 8:3059–3069.

Gard, D.L. 1992. Microtubule organization during maturation of *Xenopus* oocytes: assembly and rotation of the meiotic spindles. *Dev. Biol.* 151:516–530.

Gard, D.L., D. Affleck, and B.M. Error. 1995. Microtubule organization, acetylation, and nucleation in *Xenopus laevis* oocytes: II. A developmental transition in microtubule organization during early diplotene. *Dev. Biol.* 168:189–201.

Goshima, G., R. Wollman, N. Stuurman, J.M. Scholey, and R.D. Vale. 2005. Length control of the metaphase spindle. *Curr. Biol.* 15:1979–1988.

Gruss, O.J., and I. Vernos. 2004. The mechanism of spindle assembly: functions of Ran and its target TPX2. *J. Cell Biol.* 166:949–955.

Gruss, O.J., R.E. Carazo-Salas, C.A. Schatz, G. Guarguaglini, J. Kast, M. Wilm, N. Le Bot, I. Vernos, E. Karsenti, and I.W. Mattaj. 2001. Ran induces spindle assembly by reversing the inhibitory effect of importin alpha on TPX2 activity. *Cell.* 104:83–93.

Hetzer, M., D. Bilbao-Cortes, T.C. Walther, O.J. Gruss, and I.W. Mattaj. 2000. GTP hydrolysis by Ran is required for nuclear envelope assembly. *Mol. Cell.* 5:1013–1024.

Hodges, C.A., and P.A. Hunt. 2002. Simultaneous analysis of chromosomes and chromosome-associated proteins in mammalian oocytes and embryos. *Chromosoma.* 111:165–169.

Huchon, D., N. Crozet, N. Cantenot, and R. Ozon. 1981. Germinal vesicle breakdown in the *Xenopus laevis* oocyte: description of a transient microtubular structure. *Reprod. Nutr. Dev.* 21:135–148.

Kalab, P., R.T. Pu, and M. Dasso. 1999. The Ran GTPase regulates mitotic spindle assembly. *Curr. Biol.* 9:481–484.

Kalab, P., K. Weis, and R. Heald. 2002. Visualization of a Ran-GTP gradient in interphase and mitotic *Xenopus* egg extracts. *Science.* 295:2452–2456.

Kalab, P., A. Pralle, E.Y. Isacoff, R. Heald, and K. Weis. 2006. Analysis of a RanGTP-regulated gradient in mitotic somatic cells. *Nature.* 440:697–701.

Karsenti, E., and I. Vernos. 2001. The mitotic spindle: a self-made machine. *Science.* 294:543–547.

Kirschner, M., and T. Mitchison. 1986. Beyond self-assembly: from microtubules to morphogenesis. *Cell.* 45:329–342.

Koffa, M.D., C.M. Casanova, R. Santarella, T. Kocher, M. Wilm, and I.W. Mattaj. 2006. HURP is part of a Ran-dependent complex involved in spindle formation. *Curr. Biol.* 16:743–754.

Lefebvre, C., M.E. Terret, A. Djiane, P. Rassinier, B. Maro, and M.H. Verlhac. 2002. Meiotic spindle stability depends on MAPK-interacting and spindle-stabilizing protein (MISS), a new MAPK substrate. *J. Cell Biol.* 157:603–613.

Li, H.Y., and Y. Zheng. 2004. Phosphorylation of RCC1 in mitosis is essential for producing a high RanGTP concentration on chromosomes and for spindle assembly in mammalian cells. *Genes Dev.* 18:512–527.

Moore, W., C. Zhang, and P.R. Clarke. 2002. Targeting of RCC1 to chromosomes is required for proper mitotic spindle assembly in human cells. *Curr. Biol.* 12:1442–1447.

Nachury, M.V., T.J. Maresca, W.C. Salmon, C.M. Waterman-Storer, R. Heald, and K. Weis. 2001. Importin beta is a mitotic target of the small GTPase Ran in spindle assembly. *Cell.* 104:95–106.

Ohba, T., M. Nakamura, H. Nishitani, and T. Nishimoto. 1999. Self-organization of microtubule asters induced in *Xenopus* egg extracts by GTP-bound Ran. *Science.* 284:1356–1358.

Palacios, I., K. Weis, C. Klebe, I.W. Mattaj, and C. Dingwall. 1996. RAN/TC4 mutants identify a common requirement for snRNP and protein import into the nucleus. *J. Cell Biol.* 133:485–494.

Polanski, Z. 1986. In-vivo and in-vitro maturation rate of oocytes from two strains of mice. *J. Reprod. Fertil.* 78:103–109.

Polanski, Z. 1997. Strain difference in the timing of meiosis resumption in mouse oocytes: involvement of a cytoplasmic factor(s) acting presumably upstream of the dephosphorylation of p34cdc2 kinase. *Zygote.* 5:105–109.

Schwab, M.S., B.T. Roberts, S.D. Gross, B.J. Tunquist, F.E. Taieb, A.L. Lewellyn, and J.L. Maller. 2001. Bub1 is activated by the protein kinase p90(Rsk) during *Xenopus* oocyte maturation. *Curr. Biol.* 11:141–150.

Sillje, H.H., S. Nagel, R. Körner, and E.A. Nigg. 2006. HURP is a Ran-importin beta-regulated protein that stabilizes kinetochore microtubules in the vicinity of chromosomes. *Curr. Biol.* 16:731–742.

Silverman-Gavrila, R.V., and A. Wilde. 2006. Ran is required before metaphase for spindle assembly and chromosome alignment and after metaphase for chromosome segregation and spindle midbody organization. *Mol. Biol. Cell.* 17:2069–2080.

Szollosi, D., P. Calarco, and R.P. Donahue. 1972. Absence of centrioles in the first and second meiotic spindles of mouse oocytes. *J. Cell Sci.* 11:521–541.

Terret, M.E., C. Lefebvre, A. Djiane, P. Rassinier, J. Moreau, B. Maro, and M.H. Verlhac. 2003. DOC1R: a MAP kinase substrate that control microtubule organization of metaphase II mouse oocytes. *Development.* 130:5169–5177.

Tsurumi, C., S. Hoffmann, S. Geley, G. Ralph, and Z. Polanski. 2004. The spindle assembly checkpoint is not essential for CSF arrest of mouse oocytes. *J. Cell Biol.* 167:1037–1050.

Tulu, U.S., C. Fagerstrom, N.P. Ferenz, and P. Wadsworth. 2006. Molecular requirements for kinetochore-associated microtubule formation in mammalian cells. *Curr. Biol.* 16:536–541.

Verlhac, M.H., C. Lefebvre, P. Guillaud, P. Rassinier, and B. Maro. 2000a. Asymmetric division in mouse oocytes: with or without Mos. *Curr. Biol.* 10:1303–1306.

Verlhac, M.H., C. Lefebvre, J.Z. Kubiak, M. Umbhauer, P. Rassinier, W. Colledge, and B. Maro. 2000b. Mos activates MAP kinase in mouse oocytes through two opposite pathways. *EMBO J.* 19:6065–6074.

Whittingham, D.G. 1971. Culture of mouse ova. *J. Reprod. Fertil. Suppl.* 14:7–21.

Wiese, C., A. Wilde, M.S. Moore, S.A. Adam, A. Merdes, and Y. Zheng. 2001. Role of importin-beta in coupling Ran to downstream targets in microtubule assembly. *Science.* 291:653–656.

Wilde, A., and Y. Zheng. 1999. Stimulation of microtubule aster formation and spindle assembly by the small GTPase Ran. *Science.* 284:1359–1362.

Wollman, R., E.N. Cytrynbaum, J.T. Jones, T. Meyer, J.M. Scholey, and A. Mogilner. 2005. Efficient chromosome capture requires a bias in the 'search-and-capture' process during mitotic-spindle assembly. *Curr. Biol.* 15:828–832.

Wong, J., and G. Fang. 2006. HURP controls spindle dynamics to promote proper interkinetochore tension and efficient kinetochore capture. *J. Cell Biol.* 173:879–891.

Zhang, C., M. Hughes, and P.R. Clarke. 1999. Ran-GTP stabilises microtubule asters and inhibits nuclear assembly in *Xenopus* egg extracts. *J. Cell Sci.* 112:2453–2461.

Zheng, Y. 2004. G protein control of microtubule assembly. *Annu. Rev. Cell Dev. Biol.* 20:867–894.